# KINETICS OF CARBOXYMYOGLOBIN AND OXYMYOGLOBIN STUDIED BY PICOSECOND SPECTROSCOPY

W. G. EISERT, E. O. DEGENKOLB, L. J. NOE, AND P. M. RENTZEPIS,
*Bell Laboratories, Murray Hill, New Jersey 07974 U.S.A.*

ABSTRACT Picosecond studies of carboxymyoglobin (MbCO) and oxymyoglobin ($MbO_2$) reveal that excitation at 530 nm induces photodissociation at less than 8 ps. The kinetic and structural changes were monitored by following absorbance changes at selected wavelengths in the Soret (B) band and in the Q band. Within the 10 ps–0.45 ns period of time over which our experiments were conducted, the absorbance changes in the Soret and Q bands for MbCO and $MbO_2$ correspond to the conventional long-term, steady-state deoxymyoglobin difference spectra (Mb-MbCO and Mb-$MbO_2$), as determined by comparison of isosbestic, maximum, and minimum points. In addition, MbCO exhibits a decay to a steady state in the Soret band (monitored at 440 nm). The onset of the decay immediately follows photodissociation and has a rate of $(8 \pm 3) \times 10^9\ s^{-1}$ ($\tau = 125 \pm 50$ ps). During the 10 ps–0.45 ns observation window, relaxation is not seen for $MbO_2$ in the Soret band, nor is relaxation observed in the Q band for either MbCO or $MbO_2$. We conclude from these results that the steady state that we observe for MbCO and $MbO_2$ is most likely the stable form of deoxymyoglobin, and the relaxational differences between MbCO and $MbO_2$ observed in the Soret band indicate that the electronic destabilization after ligand detachment is very different for these molecules. We believe that these relaxational differences may be related to differences in tertiary structural changes, or due to the fact that the MbCO ($S = 0$) molecule passes through an intermediate spin Mb ($S = 1$) state before relaxing to the Mb ($S = 2$) state.

## INTRODUCTION

Most of the present day understanding of cooperativity between the subunits of hemoglobin (1, 2) has as its foundation the X-ray-determined structure of myoglobin and hemoglobin carried out by Kendrew, Perutz, and co-workers (1, 2). This cooperativity was demonstrated by the oxygen saturation (equilibrium) S-like curve and the Bohr effect (3, 4). A number of models have been proposed that attempt to explain cooperativity on some kind of molecular basis. Chronologically, these are the Monod-Wyman-Changeux (MWC) (5), the Koshland-Nemethy-Filmer (KNF) model (6), and the stereochemical model of Perutz (7). To date, the primary methods used to study cooperative effects have been Mössbauer, magnetic resonance (electronparamagnetic resonance [EPR] and nuclear magnetic resonance [NMR]), stopped-flow, and photochemical studies, carried out in a steady state of partially or fully ligated hemoglobin. Most of the photolysis investigations have monitored the

Dr. Eisert's permanent address is Institut für Strahlenbotanik, 3000 Hannover-Herrenhausen, Germany. Dr. Noe's permanent address is Department of Chemistry, University of Wyoming, Laramie, Wyo. 82071.

recombination of the sixth axial ligand, $O_2$ or CO, back onto the heme by following, under various conditions of temperature, pressure, and pH, optical density changes at suitable wavelengths as a function of time. Recently subpicosecond methods (8) and picosecond methods (9) have been used to investigate the photochemistry of heme-proteins.

The theoretical and experimental investigation of the dynamics of certain primary molecular events that precede quaternary conformational change, and thereby serve as the so-called "trigger" to cooperativity, is highly desirable. These processes include dissociation of the axial ligand and subsequent electronic and/or tertiary structural adjustments. Picosecond photodissociation experiments should prove of great value in this regard, since electronic destabilization of the heme pocket caused by ligand detachment must be followed by the evolution of electronic changes and tertiary structural changes until a stable form of the deoxyprotein results. Such evolution probably takes place before quaternary changes occur. In other words, picosecond spectroscopy is an experimental method capable of critically examining the dynamics of ultrafast molecular events in these systems, those processes serving as precursors to other extensive protein structural changes. The interpretation of the relaxation processes in hemoglobin after photodissociation is not straightforward because of the necessity of differentiating between tertiary and quaternary protein motions, and accounting for the relaxation of the individual subunits.

Since it is of interest to detect the structural events cited above, we felt that a picosecond kinetic study of carboxymyoglobin (MbCO) and oxymyoglobin ($MbO_2$) would be desirable for several reasons. First, it would provide information on protein structural and electronic relaxations immediately after photodissociation in a picosecond-subnanosecond time window, where such changes are likely to be seen. Second, the structural motions are limited to those of the tertiary type confined to one heme unit, thereby simplifying the interpretation of the effect. Finally, and perhaps most importantly, the study could provide valuable insight in conjunction with existing theory into relaxation differences between $MbO_2$ and MbCO arising from differences in electronic destabilization of the heme pocket directly after ligand detachment.

## METHODS

The sperm whale myoglobin used in this study was prepared according to the Bauer and Pacyna procedure (10). It was then saturated with CO or $O_2$ at one atmosphere and stored in pellet form (30% wt/wt) in liquid nitrogen. The samples were prepared by diluting a stock solution of melted pellets to a concentration of approximately 250 $\mu$M (4.38 mg/cm$^3$) with a mixture of tris [tris (hydroxymethyl) aminomethane] and bis-tris [bis-(2-hydroxymethyl)-imino-tris (hydroxymethyl) methane] organic buffers adjusted to pH of 7.4, ionic strength 0.022; the chloride concentration was 0.025 M. A specially designed quartz cell, 1 mm in optical path length and 3 cm high, allowed the sample to be thermostated at 5°C by circulating coolant through a quartz jacket surrounding the cell. This cell is also interconnected to a device that provides for the thermostated 5°C stock solution to be saturated with CO or $O_2$ at 1 atm. The solution in the cuvette can be periodically exchanged for fresh stock solution as the need arises.

The photodissociation of MbCo and $MbO_2$ was investigated by using a double beam $Nd^{+3}$-glass laser spectrometer originally described by Netzel and Rentzepis (11). A detailed description of the beam generation and beam geometry used for the experiments described in this report is given elsewhere (9). After sample excitation with an attenuated 530 nm, 6–8 ps pulse, the picosecond kinetics of the photodissociation and subsequent relaxation processes were monitored by following

absorbance changes from $t = 0$ to $t = 0.45$ ns at selected wavelengths in the Soret (B) band and in the Q band. Periodically we checked the photolyzed myoglobin solutions by comparing them with the original steady-state spectra, and found no evidence of denaturation, trivalent iron, or other protein damage.

## RESULTS

Although we did not deconvolute the rate of absorbance change from the temporal properties of the 530 nm excitation pulse, we can safely state that photodissociation occurs in less than 8 ps for MbCO and $MbO_2$ at the wavelengths interrogated. The absorbance change $\Delta A$ {$\Delta A$ = log [I(without excitation, $WE$)/I (with excitation; $E$)] = log [$I_0$/I($E$)]-log [$I_0$/I($WE$)]} versus wavelength (nanometers) of MbCO and $MbO_2$ are shown in Figs. 1 and 2 for time within the period 150 ps $\leq t \leq$ 450 ps after excitation. Within this period absorbance changes in the Soret and Q bands for $MbO_2$ and MbCO correspond to the conventional steady-state deoxymyoglobin difference spectra {Mb-MbCO; log [I(MbCO)/I(Mb)]} and {Mb-$MbO_2$; log [I($MbO_2$)/I(Mb)]}. This result assumes a wavelength error of ± 2 nm and takes into account the interrogation region in the Q band blanked out because of 530 nm excitation pulse interference. Table 1 establishes this correspondence by a comparison of the picosecond data to the steady-state data according to isobestic, maximum difference, and minimum difference points. The intensity maxima of

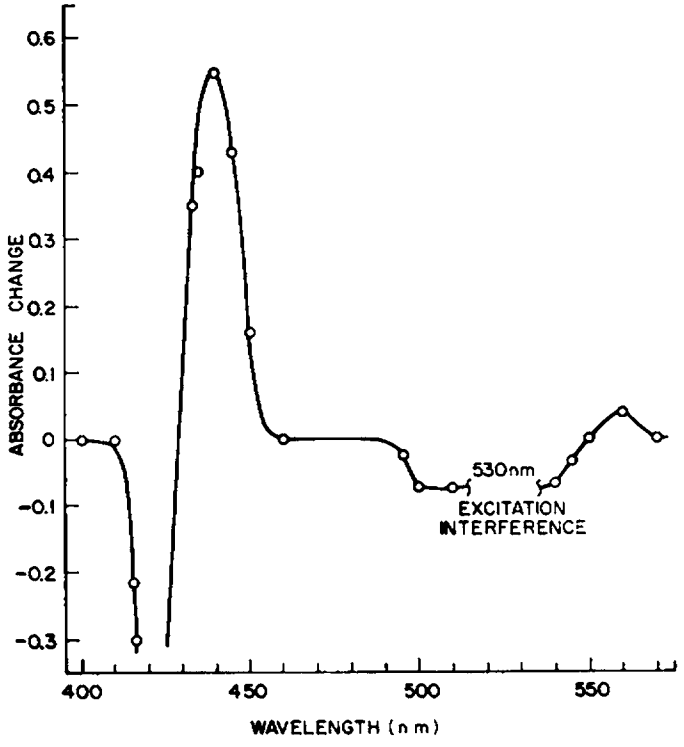


FIGURE 1 Absorbance change ($\Delta A$) vs. wavelength (nm) for MbCO between 150 ps $\leq t \leq$ 450 ps after excitation with a single 530 nm pulse. The average error of the experimental points is ± 0.03 $\Delta A$.

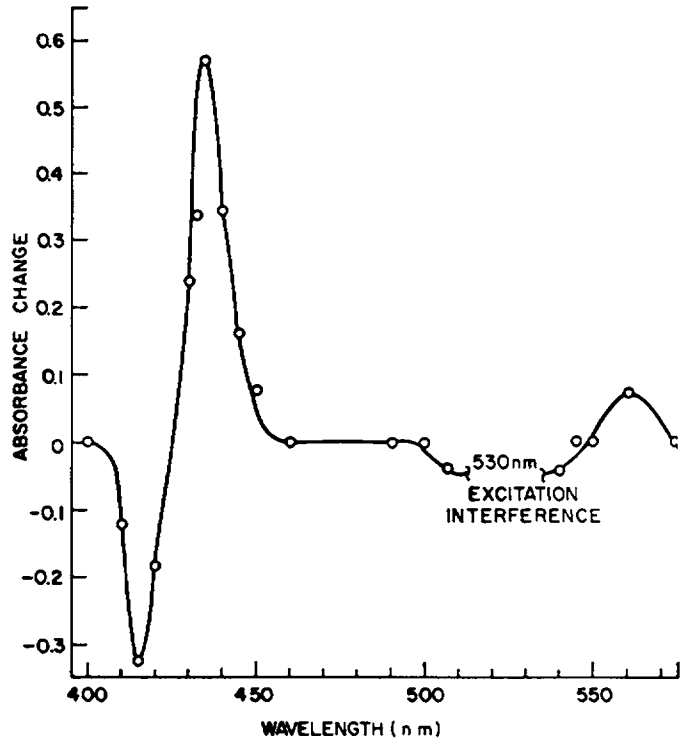


FIGURE 2 Absorbance change ($\Delta A$) vs. wavelength (nm) curve for $MbO_2$ for the period of time 150 ps $\leq t \leq$ 450 ps after excitation with a single 530 nm pulse. The average error of the experimental points is $\pm$ 0.03 $\Delta A$.

the steady-state difference spectra and the picosecond spectra agree quite well, except for the 560 nm band, where our $\Delta A$ is extremely small. For comparison, see Table I.

We also find that within the 0.02 $\Delta A$ experimental reliability, MbCO exhibits the same decay to a steady state in the Soret band, as depicted by the decay kinetics between 430 nm and 445 nm. The onset of the decay follows photodissociation and has a rate of $(8 \pm 3) \times 10^9\ s^{-1}$ ($\tau = 125 \pm 50$ ps). Taking into account our average error of $\pm$ 0.02 $\Delta A$, we do not find evidence between the 10 ps—0.45 ns observation period of relaxation or new transient states for $MbO_2$ in the Soret band, nor do we find such evidence in the Q band for either $MbO_2$ or MbCO. The absorbance ($\Delta A$) versus time (picoseconds) curves of MbCO and $MbO_2$ (for comparison) at 440 nm shown in Fig. 3 reveal this markedly different kinetic behavior. The initial peak $\Delta A$ values (about 10 ps after arrival of the excitation pulse) for MbCO and $MbO_2$, and the steady state $\Delta A$ value of MbCO after relaxation, are shown in Fig. 4 plotted against attenuated excitation energy. For $MbO_2$, $\Delta A$(peak) is the steady-state absorbance change after photodissociation. Based on the average nonattenuated single 530 nm pulse energy of 5 mJ, the linear region of these curves corresponds to attenuated excitation energies in the range $E(MbO_2) \leq 1.5$ mJ and $E$(MbCO) $\leq 0.25$ mJ.

All of our experiments, including those conducted at wavelengths other than 440 nm,

TABLE I

COMPARISON OF PICOSECOND AND STEADY-STATE DIFFERENCE SPECTRAL DATA

| Compound | λ* (Max) | λ‡ (Max) | λ* (Isosbestic) | λ§ (Isosbestic) | λ* (Max) | λ§ (Max) | λ* (Min) | λ§ (Min) |
|---|---|---|---|---|---|---|---|---|
| Soret band region, *nm* | | | | | | | | |
| Mb | 433 | 434 | | | | | | |
| $MbO_2$ | 415 | 418 | | | | | | |
| MbCO | 423 | 423 | | | | | | |
| Mb-$MbO_2$ | | | 393 | 400 | 435 | 435 | 411 | 415 |
| | | | 421 | (425) | | | | |
| | | | 458 | 460 | | | | |
| Mb-MbCO | | | 408 | 408 | | | | |
| | | | 428 | (430) | 437 | 440 | 421 | (420) |
| | | | 460 | 460 | | | | |
| Q band region, *nm* | | | | | | | | |
| Mb | 555 | 556 | | | | | | |
| $MbO_2$ | 542 | 543 | | | | | | |
| | 580 | 581 | | | | | | |
| MbCO | 540 | 542 | | | | | | |
| | 577 | 579 | | | | | | |
| Mb-$MbO_2$ | | | 508 | 500 | 517 | int | 538 | (540) |
| | | | 525 | int | 561 | 560 | | |
| | | | 547 | 547 | | | | |
| | | | 574 | 575 | | | | |
| Mb-MbCO | | | 503 | 492 | 510 | NO | 537 | (540) |
| | | | 517 | int | 558 | 560 | | |
| | | | 550 | 550 | | | | |
| | | | 570 | 570 | | | | |

| | $MbO_2$ λ(Max) | $\Delta A^*$ | $\Delta A$§ | $\Delta A^*/\Delta A$§ | MbCO λ(Max) | $\Delta A^*$ | $\Delta A$§ | $\Delta A^*/\Delta A$§ |
|---|---|---|---|---|---|---|---|---|
| | 415 | 0.33 | 0.33 | 1.00 | 420 | 0.66 | 0.60 | 1.10 |
| | 435 | 0.62 | 0.57 | 1.09 | 440 | 0.56 | 0.55 | 1.02 |
| | 560 | .03 | 0.07 | 0.43 | 560 | 0.02 | 0.025 | 0.80 |

Numbers in parentheses refer to wavelengths between data points taken from Figs. 1 and 2. int, 530 nm excitation line interference; NO, not observed. The maximum absorbance changes at 517 and 510 nm in the Q band are very small and therefore not as reliable as the Soret band data.

*Bonaventura, J., and C. Bonaventura. 1978. Private communication.

‡See ref. 29.

§Present picosecond work.

were confined to the linear-zero intercept region of these or similar saturation curves. Noble et al.[12] have determined that the quantum yield of photodissociation for MbCO ranges between 1.0 and 0.85, depending on ionic strength, protein concentration, and primary structure. The quantum yield of photodissociation of $MbO_2$ is not as well defined, but it has been assigned a value of 0.03 by Gibson and Ainsworth (13) based on $\phi$(MbCO) = 1. Taking into consideration the results of these investigators, we are reasonably sure that the nonlinear region of our saturation curves for the protein concentrations used is due to photolysis saturation, although we cannot completely rule out the possibility of multiphoton absorption process(es).

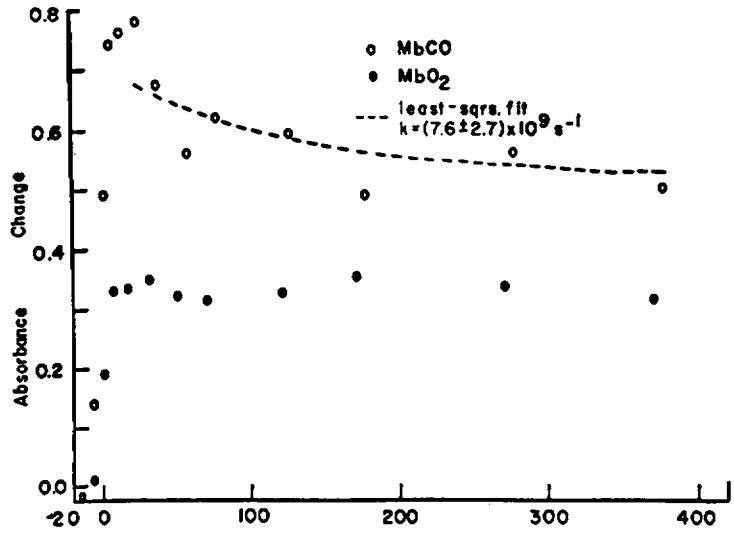


FIGURE 3 Absorbance changes in carboxymyoglobin and oxymyoglobin at 440 nm from $t = 0$ to $t =$ 376 ps after single pulse excitation at 530 nm. The curves correspond to excitation energies of 0.25 mJ and 1.6 mJ for MbCO and $MbO_2$, respectively. The average error in $\Delta A$ is $\pm$ 0.03.

## DISCUSSION

A brief survey of background information is necessary before discussing preliminary proposals to account for the observed differences in relaxation between MbCO and $MbO_2$.

The intensity and energy of the Soret and Q band transitions in myoglobin are commonly accounted for by invoking configuration interaction between the nearly degenerate ($D_{4h}$)

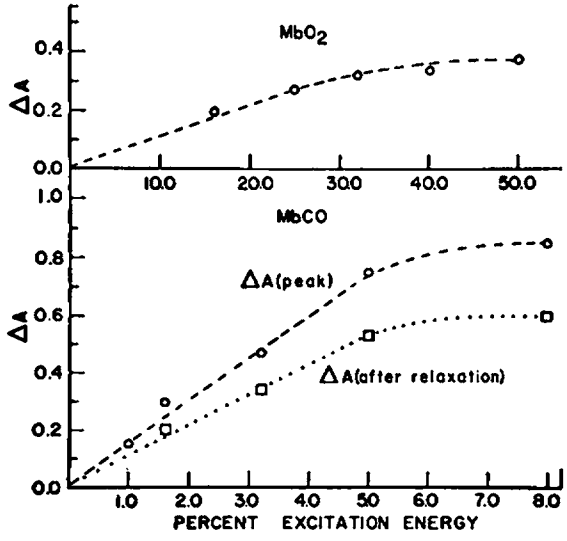


FIGURE 4 Absorbance changes (at 440 nm) vs. percent excitation energy. The upper curve is for $MbO_2$ and the lower curve is for $MbO_2$.

in-plane polarized porphyrin transitions $a_{2u}^{*}(\pi) \rightarrow e_g^{*}(\pi)$ and $a_{1u}(\pi) \rightarrow e_g^{*}(\pi)$ (14). The absorption spectrum in the Soret region is attributed to an essentially pure $\pi - \pi^*$ porphyrin transition, whereas the Q band transition is contaminated with some charge-transfer character arising from porphyrin $a_{1u}(\pi)$ and $a_{2u}(\pi)$ to iron $3d_{xz}$ and $3d_{yz}$ transitions.

The understanding of the ultraviolet-visible spectrum and photodissociation of divalent iron MbCO (and HbCO) is considerably more advanced than that of $MbO_2$ (and $HbO_2$) (15). From recent Mössbauer measurements (16), the ground state (Fe; $t_{2g}^6$) of HbCO (MbCO) was found to be about 2,000 $cm^{-1}$ below the ground state (Fe; $t_{2g}^5 e_g^1$) of $HbO_2$($MbO_2$). There is a strong possibility that this energy difference accounts for the greater affinity of Hb (or Mb) for CO than for $O_2$. In addition, the high-quantum efficiency of photodissociation of CO from divalent iron-porphyrin complexes was plausibly explained by extended Hückel calculations of Zerner et al. (14) on model porphins. Since the $a_{1g}(d_z^2)$ MO (mainly Fe) is not occupied, and therefore antibonding, a likely path for photodissociation occurs via the metal transition $e_g(d_{xz}^2, d_{yz}^2; d_\pi^4) \rightarrow a_{1g}(d_z^2)$ thought to be located in the red spectral region. This dissociative transition can in theory be accessed through a level crossing by exciting into the allowed higher-energy porphyrin Q band. If the photodissociation occurs via this transition, then triplet myoglobin could be produced with ground-state CO. The triplet state would then relax to the well-known deoxymyoglobin quintet state;

$$\mathrm{MbCO}\,(S = 0) \xrightarrow[530]{h\nu} \mathrm{Mb^*}\,(S = 1) + \mathrm{CO\,(ground)} \rightarrow \mathrm{Mb}\,(S = 2).$$

Since the bonding responsible for the low-spin $S = 2$ singlet ground state of the six coordinate $MbO_2$ is significantly different from that of MbCO (17, 18), one can quite reasonably expect the photodissociation mechanism of $MbO_2$ differs from that of MbCO. Based on earlier theoretical work on ozone and on ab initio valence bond configuration interaction calculations for $FeO_2$ and model $MbO_2$ porphins, Goddard and Olafson (17) have proposed an ozone model of $O_2$ bonding to heme. Because of its consistency with certain experimental observations, the ozone model is at variance with earlier heme—$O_2$ bonding models that notably include the 120° bent Pauling (19, 20) model (the 119° geometry predicted by the ozone model is in agreement), the coplanar ($O_2$ with the porphyrin) ring model of Griffith (21), the superoxide $Fe^{3+}$—$O_2^-$ Weiss (22) model, and the two-electron oxidative addition model of Gray (23). According to the ozone modeling, before bonding with $O_2$, the metal $Fe^{2+}$ ($C_{2v}$Mb) is in a triplet $^3E$ configuration $t_{2g}^5 e_g^1$, not the singlet $t_{2g}^6$ crystal field configuration commonly ascribed to it. The calculations further indicate that one can quite sensibly view the low-spin $S = 0$ ground state of $MbO_2$ as the triplet ground state of $O_2$ ($^3\sum_g^-$) coupled to the triplet component of the metal $t_{2g}^5 e_g^1$ configuration (hence the "ozone model"; $O(^3P) + O_2(^3\sum_g^-)$). This idea was first proposed by Eicher and Trautwein (16) from Mössbauer data. The results of the calculation are consistent with Mössbauer quadrupole splitting studies (24, 25), structural studies by Collman and co-workers (26), certain aspects of single-crystal absorption studies (15), and earlier extended Hückel calculations of Zerner et al. (14). Despite the apparent advantages of the ozone modeling for $O_2$—$Fe^{2+}$ bonding, the agreement between theory and experiment regarding the location and classification of the many optical accessible transitions in $MbO_2$, excluding the porphyrin $\pi - \pi^*$ transitions, is poor. This, in part, is due to the necessity of porphin modeling in the theoretical calculations. It is also true that the absolute experimental classification of the many possible metal $d - d$ transitions, $\pi - \pi^*$ charge-transfer transitions localized on the $O_2$, and

the metal porphyrin-$O_2$ charge-transfer transitions has not yet been accomplished. In single-crystal absorption studies, Makinen and Eaton (15) have utilized polarization ratio comparisons (and circular dichroism measurements in solution) of horse oxyhemoglobin and horse carboxyhemoglobin to distinguish certain of these charge-transfer transitions from the porphyrin $\pi - \pi^*$ background.

Considering the uncertainty in the location and in the assignment of the transitions discussed, it is not possible at the present time to propose, with any degree of certainty, a mechanism to account for the photodissociation of $O_2$ (in the $^3\sum_g^-$ state) from $MbO_2$ or $HbO_2$, the dissociation initiated by pumping a $\pi \rightarrow \pi^*$ porphyrin transition. We are reasonably certain that the $O_2$ dissociated by the 530 nm excitation pulse is in the $^3\sum_g^-$ ground state, and not in the highly reactive $O(^1D)$ or $O_2(^1\Delta_g)$ states that could arise on excitation of a high level $\pi$-charge-transfer state analogous to the Hartley band in ozone. (18).

It is clear from the calculations of Olafson and Goddard (17, 18) on four- and five-coordinate deoxymyoglobin (model porphin) complexes that nonbonded interactions play an important role in the geometry and electronic character of the heme complex. They find, in the four-coordinate porphyrin, that the optimal position of the Fe is in the plane of the porphyrin for the high spin $S = 2$ (and also for the intermediate spin $S = 1$) state, so that the attraction of Fe for the porphyrin macrocycle (that favors planar geometry) is larger than the antibonding interaction of the $d_{x^2-y^2}$ MO (that favors nonplanarity). In five-coordinate model porphin (deoxymyoglobin, Mb) they find that the complex is high spin ($S = 2$), having the same electronic configuration as the four-coordinate complex, and the principal reason for the displacement of the Fe from the porphyrin plane lies in nonbonded interactions (repulsions) between the N of the fifth ligand and the N orbitals of the porphyrin. The calculations also show that the nonbonded interactions are quite sensitive to the porphyrin ring size.

## CONCLUSIONS

Taking into account the source and magnitude of the errors discussed in the Results section, our observations strongly suggest that at times more than 0.3 ns after excitation, MbCO has relaxed to a steady state that is the same steady state that $MbO_2$ arrives at immediately after photodissociation. Furthermore, interrogation of the Soret and Q spectral regions of $MbO_2$ and MbCO selected wavelengths to 2.0 ns after excitation shows no further evidence of relaxation or spectral change. Based on the correlation of the photolysis spectra to the long-term, steady-state difference spectra, we conclude that this steady state is very likely to be the stable ($S = 2$) form of deoxymyoglobin.

The relaxation after axial ligand detachment in MbCO, and absence of relaxation in $MbO_2$, must be directly related to a redistribution of electronic charge in MbCO and absence of such redistribution in $MbO_2$, that is at least partly localized to the plane of the porphyrin dictated by the Soret band kinetics. We do not imply that no other electronic changes occur during our observation period or later. Indeed, there may be other electronic relaxations and/or transient states that are insensitive to the pure in-plane polarized $\pi - \pi^*$ Soret assay, or located at wavelengths that we have not interrogated. For example, Lindquist and associates (27), using nanosecond photolysis methods, have observed relaxations for various hemoglobins in the 50–300 ns time region by interrogation of the Soret band. They have suggested that these relaxations correspond to primary structural changes in the heme

pocket that may be associated with conformational changes. They, however, see no substantial evidence for such relaxation for either sperm whale or horse myoglobin during this time period.

Based on our conclusion that the steady state of photodissociated $MbO_2$ and MbCO (after relaxation) is highly likely to be the stable form of deoxymyoglobin Mb($S = 2$), and the facts outlined in the Discussion section leading to the conclusion that the mechanisms of photodissociation for $MbO_2$ and MbCO are certainly different, we can discuss several possible models for the observed relaxational differences between these molecules.

In the case of MbCO, which has a quantum efficiency of photodissociation defined as unity, the observed relaxation could be due to a radiationless intersystem crossing, which we record as a bleaching or depopulation, from the Mb*($S = 1$) triplet state to the stable deoxymyoglobin Mb($S = 2$) quintet state, as suggested by Zerner and associates (14). The fact that we observe this relaxation in the Soret band and not in the weaker Q band may be due to the experimental uncertainty, $\pm$ 0.03 $\Delta A$. Although the mechanism of photodissociation of $MbO_2$, which has a relatively low quantum yield, is not known, we could speculate that because of the richness of charge-transfer transistions (15), it dissociated without passing through a transient triplet that is observable with our picosecond resolution;

$$MbO_2(S = 0) \xrightarrow{\frac{h_\nu}{530}} Mb(S = 2) + O_2(^3\Sigma_g^-).$$

However, since the ground state of MbCO is thought to be 2,000 $cm^{-1}$ lower than that of $MbO_2$ (16), the electronic destabilization after ligand detachment may be reasonably expected to be greater for MbCO than for $MbO_2$. In this case our kinetic results for MbCO after photodissociation would reflect an electronic restabilization of the heme pocket, with or without the Mb*($S = 1$) state, consistent with a configurational relaxation such that a stable form of deoxyhemoglobin results. Such changes may be absent, or at least minimal, in $MbO_2$ because its binding is totally different from that of MbCO. Theoretical considerations (18) suggest that the presence or absence of relaxation assayed through an in-plane polarized $\pi - \pi^*$ porphyrin transition may be viewed in terms of an electronic stabilization of the heme pocket after photodissociation. This is caused by a balancing of attractive interactions between the iron and its ligands and repulsive nonbonded interactions between the proximal imidazole group of His H8 and the porphyrin nitrogens. Such interactions could affect the size and planarity of the porphyrin ring and thereby modulate the porphyrin $\pi - \pi^*$ absorption. Thus a primary-tertiary structural change such as a heme plane tilt could be responsible for the differences in relaxation rates between $MbO_2$ and MbCO. Supporting this model is the work of Makinen and Eaton (28), who found a difference in heme plane tilt between HbCO and $HbO_2$.

In summary, we believe that the relaxational differences observed are either due to the fact that MbCO($S = 0$) passes through a transient spin Mb*($S = 1$) state before relaxing via intersystem crossing to the stable Mb($S = 2$) state, or related to differences in tertiary structural changes confined to the heme pocket.

The authors express their appreciation to Drs. J. Bonaventura and C. Bonaventura for their valuable discussions of this manuscript and use of their unpublished data on the steady-state deoxymyoglobin difference spectra.

W.G.E. acknowledges a travel grant from the German Research Foundation.

*Received for publication 23 January 1978 and in revised form 28 October 1978.*

## REFERENCES


1. KENDREW, J. C., R. E. DICKERSON, B. E. STRANDBERG, R. G. HART, D. C. PHILLIPS, and V. C. SHORE. 1960. Structure of myoglobin. A three dimensional Fourier synthesis at 2-Å Resolution. *Nature (Lond.).* **185**:422–427.
2. PERUTZ, M. F., M. G. ROSSMANN, A. F. CULLIS, H. MUIRHEAD, G. WILL, and A. C. T. NORTH. 1960. Structure of haemoglobin. A three dimensional Fourier synthesis at 5.5 Å resolution, obtained by X-ray analysis. *Nature (Lond.).* **185**:416–422.
3. BALDWIN, J. 1975. Structure and function of hemoglobin. *Prog. Biophys. Mol. Biol.* **29**:225–329.
4. EDELSTEIN, S. J. 1975. Cooperative interactions of hemoglobin. *Annu. Rev. Biochem.* **44**:209–232.
5. MONOD, J., J. WYMAN, and J.-P. CHANGEUX. 1965. On the nature of allosteric transitions: A plausible model. *J. Mol. Biol.* **12**:88–118.
6. KOSHLAND, D. E., JR., G. NEMETHY, and D. FILMER. 1966. Comparison of experimental binding data and theoretical models in proteins containing subunits. *Biochemistry.* **5**:365–385.
7. PERUTZ, M. F. 1970. Sterochemistry of cooperative effects in haemoglobin. *Nature (Lond.).* **228**:726–739.
8. SHANK, C. V., E. P. IPPEN, and R. BERSOHN. 1976. Time-resolved spectroscopy of hemoglobin and its complexes with subpicosecond optical pulses. *Science (Wash. D.C.).* **193**:50–51.
9. NOE, L. J., W. G. EISERT, and P. M. RENTZEPIS. 1978. Picosecond photodissociation and subsequent recombination processes in carbon monoxide hemoglobin. *Proc. Natl. Acad. Sci. U.S.A.* **75**:573–577.
10. BAUER, C., and B. PACYNA. 1975. The conversion of trivalent to divalent iron in hemoglobin of various species. *Anal. Biochem.* **65**:445–448.
11. NETZEL, T. L., and P. M. RENTZEPIS. 1974. Picosecond kinetics of tetracene dianions. *Chem. Phys. Lett.* **29**: 337–342.
12. NOBLE, R. W., M. BRUNORI, J. WYMAN, and E. ANTONINI. 1967. Studies on the quantum yields of photodissociation of carbon monoxide from hemoglobin and myoglobin. *Biochemistry.* **4**:1216–1222.
13. GIBSON, Q. H., and S. AINSWORTH. 1957. Photosensitivity of haem compounds. *Nature (Lond.).* **180**:1416–1417.
14. ZERNER, M., M. GOUTERMAN, and H. KOBAYASHI. 1966. Porphyrins. VIII. Extended Hückel calculations on iron complexes. *Theor. Chim. Acta. Berl.* **6**:363–400.
15. MAKINEN, M., and W. A. EATON. 1973. Polarized single crystal absorption spectra of carboxy- and oxyhemoglobin. *Ann. N.Y. Acad. Sci.* **206**:210–222.
16. TRAUTWEIN, A., H. EICHER, A. MAYER, A. ALFSEN, M. WAKS, J. ROSA, and Y. BEUZARD. 1970. Modification of the electronic structure of ferrous iron in hemoglobin by ligandation and by alterations of the protein structure inferred from Mössbauer measurements. *J. Chem. Phys.* **53**:963–967.
17. OLAFSON, D. B., and W. A. GODDARD, III. 1977. Molecular description of dioxygen bonding in hemoglobin. *Proc. Natl. Acad. Sci. U.S.A.* **74**:1315–1319.
18. GODDARD, W. A., III, and B. D. OLAFSON. 1975. Ozone model for bonding of an $O_2$ to heme in oxyhemoglobin. *Proc. Natl. Acad. Sci. U.S.A.* **72**:2335–2339.
19. PAULING, L., and C. D. CORYELL. 1936. The magnetic properties and structure of hemoglobin, oxyhemoglobin and carbonmonoxyhemoglobin. *Proc. Natl. Acad. Sci. U.S.A.* **22**:210–216.
20. PAULING, L. 1977. Magnetic properties and structure of oxyhemoglobin. *Proc. Natl. Acad. Sci. U.S.A.* **74**: 2612–2613.
21. GRIFFITH, J. S. 1956. On the magnetic properties of some haemoglobin complexes. *Proc. R. Lond. Soc. A. Math. Phys. Sci.* **235**:23–36.
22. WEISS, J. J. 1964. Nature of the iron-oxygen bond in oxyhaemoglobin. *Nature (Lond.).* **202**:83–84.
23. GRAY, H. B. 1971. Structural models for iron and copper proteins based on spectroscopic and magnetic properties. *Adv. Chem. Ser.* **100**:365–389.
24. LANG, G., and W. MARSHALL. 1966. Mössbauer effect in some haemoglobin compounds. *J. Mol. Biol.* **18**: 385–404.
25. WEISSBLUTH, M., and J. E. MALING. 1967. Interpretation of quadrupole splittings and isomer shifts in hemoglobin. *J. Chem. Phys.* **47**:4166–4177.
26. COLLMAN, J. P., R. R. GAGNE, C. A. REED, W. T. ROBINSON, and G. S. RODLEY. Structure of an iron (II) dioxygen complex; A model for oxygen carrying hemeproteins. *Proc. Natl. Acad. Sci. U.S.A.* **71**:1326–1329.
27. ALPERT, B., R. BANERJEE, and L. LINDQUIST. 1974. The kinetics of conformational changes in hemoglobin, studied by laser photolysis. *Proc. Natl. Acad. Sci. U.S.A.* **71**:558–562.
28. MAKINEN, M. W., and W. A. EATON. 1974. Optically detected conformational change in haemoglobin single crystals. *Nature (Lond.).* **247**:62–64.
29. ANTONINI, E., and M. BRUNORI. 1971. Hemoglobin and myoglobin in their reactions with ligands. *Front. Biol.* **21**:17–20.